

Scientific Article

First Dosimetric and Biological Verification for Spot-Scanning Hadron Arc Radiation Therapy With Carbon Ions



Thomas Tessonier, PhD,^{a,b,1} Domenico Ivan Filosa, MS,^{c,d,1}
Celine Karle, MS,^{e,f,g,h,i} Filipa Baltazar, MS,^{b,f,g,h,i} Lorenzo Manti, PhD,^{c,d}
Lars Glimelius, MS,^j Thomas Haberer, PhD,^a Amir Abdollahi, PhD, MD,^{a,e,f,g,h,k}
Juergen Debus, PhD, MD,^{a,b,f,g,h,i,k} Stewart Mein, PhD,^{a,e,f,g,h,l}
Ivana Dokic, PhD,^{a,e,f,g,h} and Andrea Mairani, PhD^{a,e,m,n,*}

^aHeidelberg Ion-Beam Therapy Center, Department of Radiation Oncology, Heidelberg University Hospital, Heidelberg, Germany; ^bClinical Cooperation Unit Radiation Oncology (E050), German Cancer Research Center, Heidelberg, Germany; ^cRadiation Biophysics Laboratory, Department of Physics “E. Pancini,” University of Naples Federico II, Naples, Italy; ^dIstituto Nazionale di Fisica Nucleare-INFN, Sezione di Napoli, Naples, Italy; ^eClinical Cooperation Unit Translational Radiation Oncology (E210), National Center for Tumor Diseases, Heidelberg University Hospital and German Cancer Research Center, Heidelberg, Germany; ^fDivision of Molecular and Translational Radiation Oncology, Department of Radiation Oncology, Heidelberg Faculty of Medicine and Heidelberg University Hospital, Heidelberg Ion-Beam Therapy Center, Heidelberg, Germany; ^gGerman Cancer Consortium Core-Center Heidelberg, German Cancer Research Center, Heidelberg, Germany; ^hNational Center for Radiation Oncology, Heidelberg Institute of Radiation Oncology, Heidelberg University and German Cancer Research Center, Heidelberg, Germany; ⁱDepartment of Physics and Astronomy, Heidelberg University, Heidelberg, Germany; ^jRaySearch Laboratories, Stockholm; ^kDepartment of Radiation Oncology, Heidelberg University Hospital, Heidelberg, Germany; ^lDepartment of Radiation Oncology, University of Pennsylvania, Philadelphia, Pennsylvania; ^mNational Center for Tumor Diseases, Heidelberg, Germany; and ⁿNational Centre of Oncological Hadrontherapy, Medical Physics, Pavia, Italy

Received 18 February 2024; accepted 28 June 2024

Purpose: Spot-scanning hadron arc radiation therapy (SHArc) is a novel delivery technique for ion beams with potentially improved dose conformity and dose-averaged linear energy transfer (LET_d) redistribution. The first dosimetric validation and in vitro verification of carbon ion arc delivery is presented.

Methods and Materials: Intensity-modulated particle therapy (IMPT) and SHArc plans were designed to deliver homogeneous physical dose or biological dose in a cylindrical polymethyl methacrylate (PMMA) phantom. Additional IMPT carbon plans were optimized for testing different LET_d-boosting strategies. Verifications of planned doses were performed with an ionization chamber, and a clonogenic survival assay was conducted using A549 cancer lung cell line. Radiation-induced nuclear 53BP1 foci were assessed to evaluate the cellular response in both normoxic and hypoxic conditions.

Results: Dosimetric measurements and clonogenic assay results showed a good agreement with planned dose and survival distributions. Measured survival fractions and foci confirmed carbon ions SHArc as a potential modality to overcome hypoxia-induced

Sources of support: This work was supported by intramural funds from National Center for Tumor diseases (NCT3.0_2015.21/22 NCT-PRO and Biodose programs). The funders had no role in study design, data collection and analysis, decision to publish or preparation of the manuscript.

Research data are stored in an institutional repository and will be shared upon request to the corresponding author.

¹T.T. and D.F. contributed equally to this work.

*Corresponding author: Andrea Mairani; Email: Andrea.Mairani@med.uni-heidelberg.de

<https://doi.org/10.1016/j.adro.2024.101611>

2452-1094/© 2024 Published by Elsevier Inc. on behalf of American Society for Radiation Oncology. This is an open access article under the CC BY-NC-ND license (<http://creativecommons.org/licenses/by-nc-nd/4.0/>).

radioresistance. LET_d-boosted IMPT plans reached similar LET_d in the target as in SHArc plans, promising similar features against hypoxia but at the cost of an increased entrance dose. SHArc resulted, however, in a lower dose bath but in a larger volume around the target.

Conclusions: The first proof-of-principle of carbon ions SHArc delivery was performed, and experimental evidence suggests this novel modality as an attractive approach for treating hypoxic tumors.

© 2024 Published by Elsevier Inc. on behalf of American Society for Radiation Oncology. This is an open access article under the CC BY-NC-ND license (<http://creativecommons.org/licenses/by-nc-nd/4.0/>).

Introduction

Spot-scanning hadron arc (SHArc) radiation therapy, the first arc delivery technique for light and heavy ions, was introduced in silico for proton, helium, carbon, oxygen, and neon ion beams¹⁻³ offering potential treatment benefits such as increased normal tissue sparing from higher doses, possible enhanced target dose-averaged linear energy transfer (LET_d), and potential reduction in high-LET_d components in organs at risk (OARs). Development of treatment planning and optimization is ongoing at the Heidelberg Ion-Beam Therapy Center (HIT), with initial in silico studies. SHArc therapy could be delivered with either an isocentric gantry or with a gantry-less approach using a rotating chair for treatment in an upright position.⁴ For carbon ions SHArc, LET_d was predicted to increase in the target volume from ~40 keV/μm to ~80-140 keV/μm compared with conventional carbon ions delivery.¹ Moreover, favorable LET_d distributions were possible with the SHArc approach, with maximum LET_d in clinical target volume (CTV)/gross tumor volume (GTV) and potential reductions of high-LET_d regions in normal tissues and OARs. Compared with photon volumetric arc therapy, SHArc affords substantial reductions in dose to the normal tissue (40%-70%).²

Tumor hypoxia can significantly diminish the response to radiation therapy,^{5,6} because of reduced production of reactive oxygen species and consequently in DNA damage, leading to a poorer prognosis. High-LET radiation can increase cell killing of hypoxic tumors compared with low-LET radiation (eg, photons and protons) via induction of more complex DNA damage, resulting in an increased relative biological effectiveness (RBE).⁷ Thus, theoretically, high-LET carbon ions delivery should allow efficient cell killing independently of the oxygen status.⁸ In reality, however, current clinical planning and delivery standards for intensity-modulated particle therapy (IMPT)^{1,9} using carbon ions do not yield high enough LET in the tumor to efficiently eradicate the hypoxic niche. More specifically, LET_d values in patient treatment typically reach values up to 30-50 keV/μm, which can be considered low- to mid-range values, with a strong dependency on the tumor volume and beam arrangements. Higher LET_d levels (≥ 100 keV/μm for carbon ions) are found mostly in the distal edge of the tumor and/or in the surrounding healthy tissues.^{1,9} Therefore, LET_d-boosting

strategies in the target may be necessary to overcome tumor radioresistance factors like hypoxia.^{10,11} Novel approaches are emerging with the intent to effectively boost LET_d in the target, such as LET_d-optimization for IMPT plan with heavy ions as recently introduced in a commercial treatment planning system (TPS),¹² carbon ion arc therapy, or multi-ion therapy strategies combining lower and higher LET particles.^{13,14}

Recent works have developed proton arc delivery with existing gantry systems as proof of concept toward the first prototype system.¹⁵ Others have built a dedicated rotational staging system for dosimetry and radiobiological investigations using a fixed-beam setup.¹⁶ The biological investigations have been limited to proton therapy and have shown increased RBE as a function of LET for clinically relevant distributions. To date, there are no studies that demonstrate the arc delivery system for other ions such as helium and carbon.

In this work, a dedicated rotational system was developed for investigating the feasibility and efficacy of arc delivery, mimicking upright position treatment, at a synchrotron-based facility for light and heavy ions, through dosimetry and biological studies. Planning and dosimetry for arc versus conventional IMPT were performed for carbon ions. In vitro study with a tumor cell line was carried out. Additionally, tumor cells in hypoxia have been irradiated, showcasing the capability of carbon ions SHArc to eradicate hypoxic tumor cells while keeping a reasonably low-dose bath, thus potentially widening the therapeutic window in carbon ion therapy. SHArc plans have been additionally compared in silico against IMPT strategies aiming to increase LET_d in the target, in a phantom and an exemplary glioblastoma patient.

Methods and Materials

Experimental setup

A cylindrical polymethyl methacrylate phantom (20 cm in diameter) was used for the first dosimetric and in vitro biological verification of arc delivery with carbon ions (Q1/Q2 2023 at HIT). Four inserts were made in the phantom (Fig. 1A, B) in order to allocate the ionizing chamber (Pin-Point-TM31015 chamber, PTW) for dose verification and 2-mL tubes (Eppendorf) for cell irradiation (Fig. 1B). A

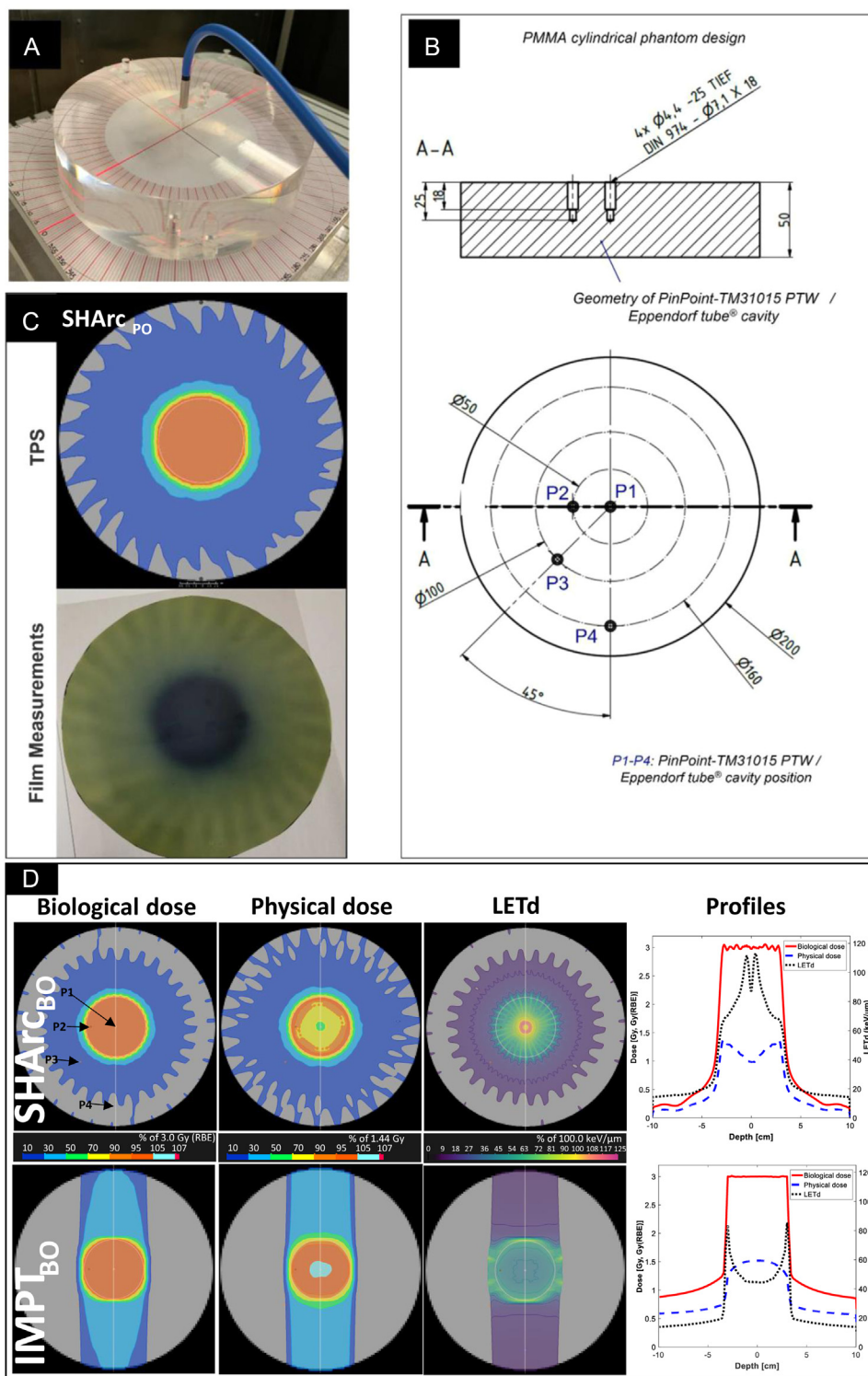


Figure 1 (A) Experimental setup with rotational stage and polymethyl methacrylate (PMMA) phantom with inserts for PinPoint-TM31015 chamber (PTW) chambers and Eppendorf tubes. (B) Schematic of the phantom, depicting insert geometry and measurement positions P1-P4. (C) Screenshots of a representative carbon SHArc generated plan (physically optimized) and corresponding film measurements. (D) SHArc and IMPT carbon ions biologically optimized plans. The optimization goal was 3 Gy (RBE) in the planning target volume (PTV, marked with an orange line). The resulting biological dose, physical dose and LET_d distributions are displayed. Profiles are also shown for the positions indicated with lines on the 2D distributions. The arrows labeled as P1, P2, P3, and P4 indicated the positions for dose and biological measurements.
 Abbreviations: IMPT = intensity-modulated particle therapy; LET_d = dose-averaged linear energy transfer; SHArc = spot-scanning hadron arc therapy; TPS = treatment planning system.

positioning stage was used, which was rotating between 2 consecutive particle delivery (spill). At HIT, the pause between each spill is about 3 to 4 seconds.¹⁷

Planning of IMPT and SHArc plans in a cylindrical phantom

The treatment plans for carbon ions delivery in the horizontal room were designed and optimized for both SHArc and opposing 2-field arrangement with the clinical TPS RayStation 11B (RaySearch Laboratories). The planning target volume was a cylinder of 3 cm radius and 4 cm height centered at the isocenter.

First, plans were optimized to ensure a uniform and conformal physical dose within the target of 1, 2, and 6 Gy with standard IMPT (physically optimized IMPT, IMPT_{PO}) or with SHArc (physically optimized SHArc, SHArc_{PO}). The aim was to verify dosimetrically the SHArc_{PO} (IMPT_{PO}) delivered plans, as well as to validate *in vitro* microdosimetric kinetic model (mMKM) based biological predictions in the TPS.^{18,19} For SHArc_{PO}, the plan consisted of 90 carbon ions beams separated every 4° over a 360° arc, with 1 energy chosen per angle. Three energies have been used, repeating every 12°: 254.71, 257.00, and 259.29 MeV/u (range in water of 12.5, 12.7, and 12.9 cm, respectively) for carbon ions. For IMPT_{PO}, 2 opposite fields were used covering the entire target, and the energy slices ranged from 205.60 to 284.84 MeV/u (range in water, 8.5-15.2 cm). Delivery time was about 7 minutes for both the investigated delivery techniques. As initial verification of the setup and delivery feasibility, the polymethyl methacrylate phantom with a radiochromic film (Gafchromic EBT film, Advanced Materials Group, International. Specialty Products) (Fig. 1C) was irradiated with the 6 Gy SHArc_{PO} plan. An additional plan considering an organ at risk and its film verification is presented in Figure E1. Second, biological dose (RBE-weighted dose) optimization was performed achieving a biological dose of 3 Gy (RBE) in the planning target volume for both SHArc (biologically optimized SHArc, SHArc_{BO}) and IMPT (biologically optimized IMPT, IMPT_{BO}) as shown in Fig. 1D. For SHArc_{BO}, the plan consisted of 90 carbon ions beams separated every 4° over a 360° arc, with 1 energy per angle and alternating energy layers at each angle of 244.21, 246.57, and 248.91 MeV/u (range in water of 11.6, 11.8, and 12.0 cm, respectively). Every 12° the same energy is used. A slight energy shift compared with the SHArc_{PO} was applied (range difference of about -0.9 cm) to increase the LET_d further in P1 for SHArc_{BO}. For IMPT_{BO}, the energy layers ranged from 205.60 to 284.84 MeV/u (range in water, 8.5-15.2 cm). The numbers of particles for the IMPT_{BO} and SHArc_{BO} were 1.46×10^9 and 1.48×10^9 . Delivery time was about 7 minutes for both the investigated delivery techniques. The

LET_d increase in the SHArc plan was ensured through the energy selection, with the Bragg peak of each energy layer finishing near the center of the phantom. In comparison, the IMPT plan energy layers are covering the whole target for each beam. The resulting biological dose, physical dose, and LET_d distributions are shown in Fig. 1D for carbon ions SHArc_{BO} and IMPT_{BO}. Verifications of SHArc_{BO} and IMPT_{BO} dosimetric and biological predictions were performed. Additionally, carbon ions SHArc_{BO} and IMPT_{BO} plans were delivered in hypoxic conditions.

Three additional approaches were investigated *in silico* and are presented in the [Supplementary Materials](#): 2 biological dose LET_d-boosted carbon ions IMPT optimizations and 1 LET_d-boosted SHArc.

Dosimetric verification of the experimental plan

The physically and biologically optimized SHArc (SHArc_{PO} and SHArc_{BO}) and IMPT (IMPT_{PO} and IMPT_{BO}) plans were verified with a PinPoint-TM31015 ionization chamber at positions P1-P4 (Fig. 1B) following clinical protocols.²⁰ Films have been used as the initial qualitative verification method of the entire workflow (Fig. 1C and Figure E1).

Cell culture and experimental *in vitro* validation

Human lung epithelial cells A549 (p53 wild-type adenocarcinoma; ATCC) were cultured in Dulbecco modified Eagle medium, supplemented with 10% heat-inactivated fetal bovine serum (Millipore) and 1% penicillin/streptomycin (Thermo Fisher Scientific) at 37°C at 5% CO₂ and 21% O₂. Prior to the irradiations with carbon ions, the parametrization from x-ray irradiation of the mMKM inputs used in the TPS was performed and is presented in the [Supplementary Material](#) and Figure E2. For the cell irradiation setup inside the phantom for carbon ion beam irradiation, the cells resuspended in 1 mL of medium were added to the 2-mL tubes (Eppendorf) and centrifuged at 1000 rpm for 5 minutes to ensure the cell pellet was correctly located at the bottom during irradiation. The tubes were then sealed with perforated parafilm to prevent medium leakage while ensuring gas exchange. The cells were then incubated in either 21% O₂ in an incubator or 1% O₂ using an *in-cubator* hypoxia chamber (C-chamber; Biospherix) for 3 hours before the irradiation. The hypoxia chamber controller allowed for the monitoring and control of CO₂ and O₂ concentrations (ProOx and ProCO2 model; Biospherix) prior to irradiation. To verify hypoxia status of the medium within the Eppendorf tubes, a Greisinger GOX 100 oxygen sensor was inserted directly

prior to irradiation. At the time of irradiation, $p\text{O}_2$ values were $\sim 21\%$ and $\sim 1.0\%$ for the normoxic and hypoxic samples, respectively. After irradiation, the cells were seeded in 25-cm^2 flasks (triplicates) and incubated for 5 days at 37°C at $21\% \text{O}_2$ and $5\% \text{CO}_2$. Nonirradiated cells under the same environmental conditions were used as controls. After colonies were formed, these were fixed with 75% methanol and 25% acetic acid for 10 minutes at room temperature and stained with 0.1% crystal violet for 10 minutes. Colonies containing more than 50 cells were counted as survivors.

All in vitro experiments were performed in triplicates 3 times; the results are given as mean values and standard error of the mean. Statistical comparison between outcomes in hypoxic and normoxic conditions was performed using a 2-tailed unpaired Student t test with significance level α set to 0.05.

Planning of IMPT and SHArc plans for an exemplary glioblastoma patient

An anonymized recurrent glioblastoma patient was taken as proof of principle for comparing different planning strategies. In this work, the biological dose was planned at 51 Gy (RBE) in 17 fractions. The IMPT plan was optimized with 2 opposite beams covering the whole target. The IMPT LET_d -optimized plan (IMPT_{LET}) used the same beams as in standard IMPT, but adding a LET_d -optimization function to the GTV to reach $80 \text{ keV}/\mu\text{m}$. The SHArc plan was optimized for 20 beams (every 18°) over a 360° arc. Each beam was planned for 5 energies, separated by 3 mm depth, distributed over the center of the target in the beam eye view. For the LET_d -optimized SHArc plan, the same beams and energies were used, but adding a LET_d -optimization function to the GTV to reach $80 \text{ keV}/\mu\text{m}$. A robust evaluation of the CTV and GTV coverage was carried out, considering 3 mm position (14 positions) and 3% range (step of 1.5%) uncertainties. An additional evaluation for 3 mm position and 1.5% range uncertainties was also made assuming the possibility of performing planning based on dual-energy CT images, reducing uncertainties on stopping power ratio value estimation.²¹ Seventy and 42 scenarios were generated for the 2 evaluations, respectively.

Results

Dosimetry

Dosimetric results for IMPT and SHArc plans for carbon ions are summarized in Table 1. An exemplary dose map of the SHArc_{PO} plan and the IMPT_{BO} as well as SHArc_{BO} are displayed in Fig. 1. A video of the 7-minute entire irradiation of a SHArc_{PO} plan (with a speed-up

Table 1 Dosimetric summary for carbon ions IMPT and SHArc plans

Optimization	Planning modality	Position name: LET_d (keV/ μm)	Dose agreement: planned vs measured (mean \pm SD)
Physical	IMPT _{PO}	P1: 34.3	$-0.1\% \pm 0.4\%$
		P2: 38.4	$2.0\% \pm 0.6\%$
		P3: 30.6	$-0.2\% \pm 0.2\%$
		P4: 14.6	$-0.5\% \pm 0.1\%$
	SHArc _{PO}	P1: 37.4	$-0.3\% \pm 0.2\%$
		P2: 55.6	$-1.7\% \pm 0.6\%$
		P3: 18.1	$-2.4\% \pm 0.3\%$
		P4: 14.8	$-0.2\% \pm 0.2\%$
Biological	IMPT _{BO}	P1: 44.6	$-0.4\% \pm 0.3\%$
		P2: 50.3	$0.9\% \pm 0.4\%$
		P3: 27.9	$-2.5\% \pm 0.9\%$
		P4: 14.7	$0.2\% \pm 0.5\%$
	SHArc _{BO}	P1: 87.3	$-0.2\% \pm 0.9\%$
		P2: 54.5	$7.9\%^* \pm 2.1\%^*$
		P3: 18.5	$2.2\% \pm 0.3\%$
		P4: 15.5	$3.9\% \pm 1.2\%$

*Indicates measurement in a large dose gradient.

Planning modality and corresponding LET_d values at the measurement point are reported. Following clinical QA procedure, the measured-to-calculated dose difference, normalized to the maximum calculated beam dose, was adopted as the main dosimetric evaluator.²⁰ The standard deviation has been calculated from multiple (at least 3) repeated chamber measurements.

Abbreviations: IMPT = intensity-modulated particle therapy; SHArc = spot-scanning hadron arc therapy.

factor of ~ 8) is available in the [Supplementary Material](#). The corresponding LET_d values in $\text{keV}/\mu\text{m}$ at the measurement positions (P1-P4) are also reported. Following the clinical quality assurance (QA) procedure, the measured-to-calculated dose difference, normalized to the maximum calculated beam dose, ΔD_{max} was adopted as the main dosimetric evaluator.²⁰ The mean and standard deviation of ΔD_{max} for all the investigated plans is shown in the last column of Table 1. For the central position, mean ΔD_{max} was below 1% for both IMPT_{PO} and SHArc_{PO} plans with variations up to 2.5% in other positions. Additionally, for SHArc_{BO} and IMPT_{BO}, mean ΔD_{max} values were 3.5% and -0.5% , respectively, as reported in Table 1 together with corresponding LET_d values.

The results of an in silico comparison of the features of different planning strategies, in terms of RBE-weighted dose, LET_d , and corresponding dose volume histograms (DVH) and LET_d volume histograms (LVH), are presented in [Supplementary Materials](#).

In vitro verification of IMPT and SHArc plans

In Fig. 2, in vitro verification of the IMPT_{PO} and SHArc_{PO} plans for both beam modalities is shown for the

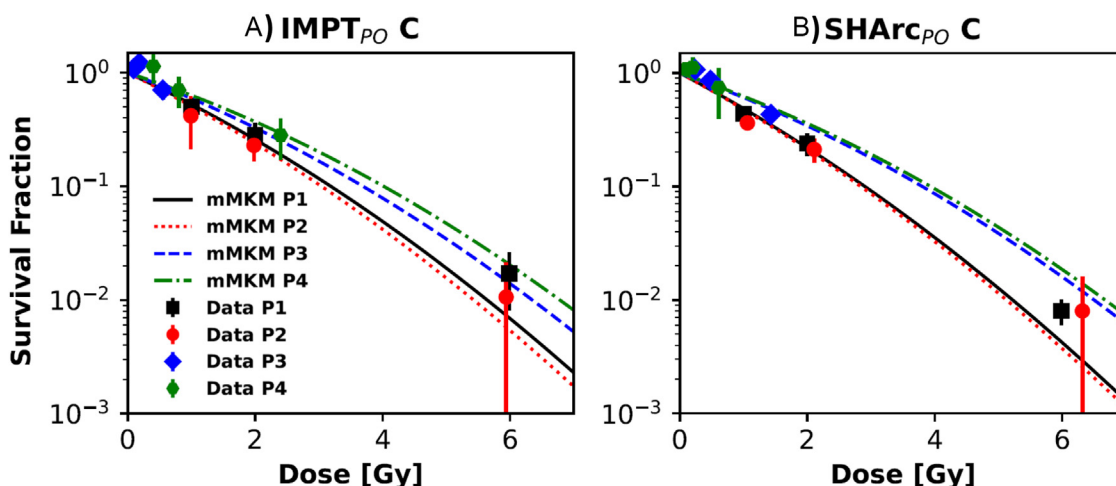


Figure 2 In vitro validation of the clinical treatment planning system (TPS) to predict cell survival as function of dose for IMPT_{PO} (A) and SHArc_{PO} (B) plans with carbon ions. Microdosimetric kinetic model (mMKM)-based TPS predictions are depicted with lines for measurement positions P1, P2, P3, and P4 while experimental data are shown as points with error bars. *Abbreviations:* IMPT = intensity-modulated particle therapy; SHArc = spot-scanning hadron arc therapy.

4 measurement positions (P1-P4). In general, model predictions match the experimental data for both beam delivery approaches. Quantitatively, considering P1 and P2, that is, the positions with larger dose spans, the mean relative differences between the measured and predicted logarithm of survival fraction were 1.3% and 2.2% for IMPT_{PO} and SHArc_{PO}, respectively.

The in vitro verification of the biologically optimized plans depicted in Fig. 1D was performed to assess the difference between measured and expected survival values for P1 and P2. IMPT_{BO} expected and measured survival fractions were 0.34 (0.35) and 0.36 ± 0.02 (0.36 ± 0.03) for P1 (P2), whereas for SHArc_{BO}, they were 0.35 (0.36) and 0.35 ± 0.07 (0.40 ± 0.10) for P1 (P2).

The results of the in vitro measurements in P1 for the biologically optimized carbon ions plans (SHArc_{BO} and IMPT_{BO}) in either normoxia (O₂~21%) or hypoxic conditions (O₂~1%) are presented in Fig. 3. Clonogenic survival assay results are presented in Fig. 3A, B. When comparing irradiations under normoxic and hypoxic conditions, IMPT_{BO} showed a statistically significant increase in radioresistance in hypoxic compared with normoxic conditions ($P = .004$), whereas SHArc_{BO} kept a similar level of cytotoxicity ($P = .4942$). This was additionally confirmed by comparing the radiation-induced nuclear 53BP1 foci at 30 hours postirradiation as shown in Fig. 3C, D. Higher survival fraction of IMPT_{BO} in hypoxia was correlated with a lower amount of remaining 53BP1 signals at 30 hours. The ratios between the average number of 53BP1 foci per nucleus in hypoxic conditions and that in normoxic conditions are about 2.0 ± 0.5 and 0.8 ± 0.2 for IMPT_{BO} and SHArc_{BO} irradiations, respectively. Representative images for IMPT_{BO}- and SHArc_{BO}-induced nuclear 53BP1 foci at 30 hours postirradiation are shown in Figure E3.

Comparison of carbon ions RBE-weighted dose optimization strategies on an exemplary glioblastoma patient

The resulting biological dose and LET_d distributions, and correspondent DVH and LVH are shown in Fig. 4. LVH and DVH metrics are extracted and presented in Table E2. The LET_d-optimized IMPT plan and both SHArc plans exhibit high-LET_d values in the GTV (LET_{mean} >80 keV/μm), compared with the clinical IMPT plan (LET_{mean} of 60 keV/μm). However, the dose in the brain (without CTV with a 3 mm margin) presents higher dose components in the LET_d-optimized IMPT plan, as highlighted by the line dose profile. Both SHArc plans present a LET_d redistribution inside the target volume, the LET_d-optimized SHArc plan allows an optimal redistribution within the GTV (LET_{d98%} ~ 81 keV/μm for the LET_d-optimized plan against 46 keV/μm for the classic SHArc plan). Similar to phantom results, SHArc plans yielded in the patient the lowest LET_{d2%} in the brain, down to 67 keV/μm compared with 93 keV/μm for IMPT techniques. In terms of robustness against position and range uncertainties, the clinical IMPT approach yields superior results for target coverage compared with the other strategies (Table E3).

Discussion

The first dosimetric and in vitro evaluation of arc delivery with carbon ions was performed, and the potential of high-LET_d arc delivery with carbon ions to overcome hypoxia-induced radiation resistance has been

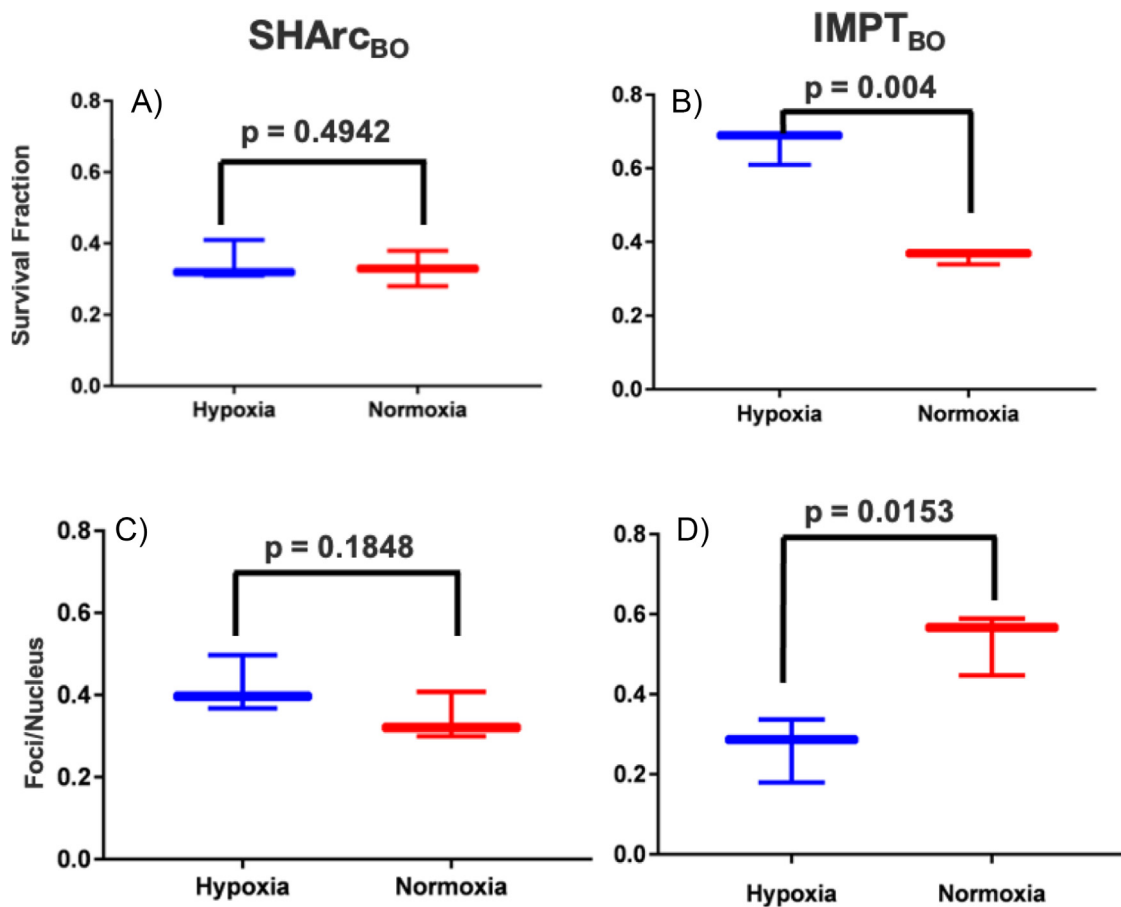


Figure 3 (A, B) Survival fraction of A549 cells irradiated with SHArc_{BO} (A) or IMPT_{BO} (B) in normoxia and hypoxia. (C, D) 30 hours postirradiation 53BP1 foci per nucleus in hypoxic and normoxic conditions after SHArc_{BO} (C) or IMPT_{BO} (D) delivery. The *P* values are also reported.

Abbreviations: IMPT = intensity-modulated particle therapy; SHArc = spot-scanning hadron arc therapy.

demonstrated. This key feature of carbon ions SHArc delivery could bring new possibilities to the clinic for the treatment of hypoxic tumors, with the drawback of presenting a low-dose bath in the patient but without increasing the maximum dose in the target surrounding normal tissues or beam entrance ports. For this purpose, a framework mimicking upright treatment with a fixed beamline was introduced, delivering SHArc plans to perform their verification dosimetrically as well as radiobiologically in vitro. The setup used could serve as preclinical verification for future deployment of arc delivery with upright positioning using, for example, the system provided by Leo Cancer Care.

SHArc plans were successfully optimized, and they are presenting a particular shape in their dose/LET_d distributions as seen in Fig. 1C, D. The “peak” and “valley” structures shown in the LET_d and dose distributions at the outward periphery of the phantom are linked to the optimization process and the objective to achieve a homogeneous dose distribution. The density of the Bragg peak positions, coming from the 90 angles, is higher in the center of the phantom compared with the outer regions of

the target, owing to the prior energy selection to have a high-LET_d in the core center of the target and the shape of the phantom. Thus, during optimization of physical and biological plans, the weights of these central spots are reduced in order to achieve a homogeneous distribution, leading to a decrease in dose/LET_d.

Dosimetric verification of SHArc_{PO}, IMPT_{PO}, and IMPT_{BO} showed excellent results, whereas for carbon ions SHArc_{BO}, mean ΔD_{max} was 3.5%. Excluding measurements (P2) with a large dose gradient (>0.04 Gy/mm), similarly as performed during clinical QA, resulted in a mean ΔD_{max} of 2.0%. The obtained results confirmed the capability of the delivery system to irradiate an arc plan generated using a clinical TPS. A limitation of this study is that we have employed a simple homogeneous cylindrical phantom for the dosimetric verification of the plans with 90 beams. Additional dosimetric studies should be performed using anthropomorphic phantoms, with fewer angles but more energy layers per angle.

In terms of biological measurements, the IMPT_{PO} and SHArc_{PO} plans were used to irradiate human lung epithelial cells A549 to benchmark RBE predictions based on

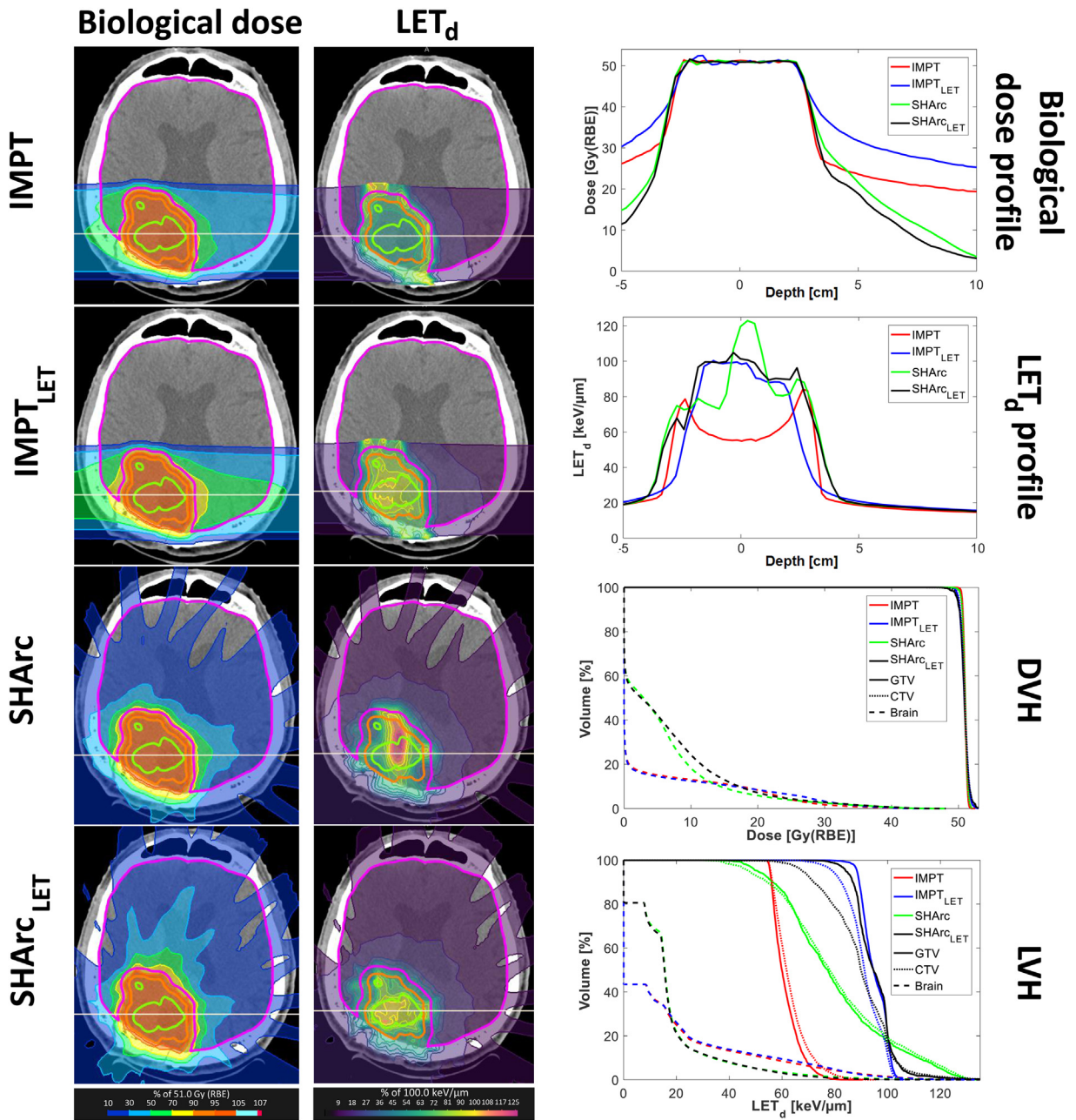


Figure 4 Exemplary glioblastoma patient treatment with different delivery strategies: IMPT, LET_d-optimized IMPT (IMPT_{LET}), SHArc, and LET_d-optimized SHArc (SHArc_{LET}). Biological dose and LET_d profiles are displayed as well as biological dose and LET_d volume histograms (DVH, LVH) with the gross target volume (GTV, yellow in the patient distributions), clinical target volume (CTV, orange in the patient distributions), and Brain (without CTV with 3-mm margins, pink in the patient distributions).

Abbreviations: IMPT = intensity-modulated particle therapy; LET_d = dose-averaged linear energy transfer; SHArc = spot-scanning hadron arc therapy; DVH = Dose volume histograms; LVH = LET_d volume histograms.

mMKM and verify the experimental setup for in vitro verification. In general, mMKM predictions were in good agreement with cell survival as shown in Fig. 2. However, for carbon ions at high dose levels (6 Gy) for P1 and P2 positions, mMKM tends to overestimate cell killing, which warrants testing of updated mMKM versions²² that have been introduced to better describe the β term for higher LET particles.

The number of particles for the IMPT_{BO} and SHArc_{BO} were 1.46×10^9 and 1.48×10^9 , that is, with no substantial difference between the 2 delivery approaches. As shown in previous works,^{1–3} SHArc plan attributes, such as the number of particles, are influenced by the selected RBE model and associated inputs (eg, tissue type) as well as selected arc trajectory (partial or full arc), target size, and optimization strategy (number of energy per angles, angle numbers).

In terms of delivery time, SHArc plans took about 7 minutes, and thus, a small step in energy layer spacing for IMPT plans was used (2 mm distance between each energy layer position in water instead of the 3 mm used in clinical practice) to increase the number of total energies per beam, achieving a similar total delivery time. This allows reducing potential differences in dose rate, which could influence the biological effect (especially for lower LET components). Developments are in progress at our synchrotron-based facility to integrate more efficient delivery methods that would allow delivery of more than 1 energy per spill, as already investigated in other centers.^{23–25}

In order to keep a reasonable delivery time, the delivered SHArc_{BO} plans used only 1 energy per angle, for a total of 3 energies for the 90 angles, to slightly extend the Bragg peak positions in the phantom and to be less sensitive to range uncertainties. Using more energies, even with fewer angles, could allow to reduce further range uncertainties, increase the dose homogeneity, and distribute more homogeneously the high-LET_d component as seen in the comparison of the optimization strategies between SHArc_{BO} and SHArc_{LET}.

The SHArc_{BO} plan presents a central core of 3 cm diameter receiving $>75\text{ keV}/\mu\text{m}$ and $>89\text{ keV}/\mu\text{m}$ for the inner 2 cm diameter core, whereas the IMPT_{BO} plan received in this region a relatively homogeneous $45\text{ keV}/\mu\text{m}$. Such high-LET_d in the inner core of the target could be suitable to overcome hypoxia-related radioresistance and is highlighted by the results of the hypoxia experiments. SHArc_{BO} plan was isoeffective in killing in the central region of the target, in both normoxia and hypoxia, whereas the effectiveness of the IMPT_{BO} plan is largely reduced in hypoxia as shown in the upper panels of Fig. 3. This was also confirmed by looking at the 30-hour postirradiation ratios of 53BP1 foci per nucleus in hypoxic and normoxic conditions applying the 2 delivery approaches. All the LET_d-boosting strategies presented in [Supplementary Materials](#), with IMPT or SHArc, should result in similar isoeffective killing of the radioresistant cells, according to the LET_d value found in the inner core. Among these plans, the LET_d-boosted SHArc, with a reduced number of angles but more energies per angle, even increased the SHArc plan's ability to create a homogeneous biological dose in the target as well as, through LET_d-optimization, a more uniform high-LET_d within its central core, that was not achievable with a single energy per angle approach.

The oxygen level in the samples seemed to be relatively stable (around 1%) in the cell environment as measured with an oxygen sensor (OxyLite, Oxford Optronix) and confirmed indirectly by the reproducibility of experiments in hypoxic conditions.

The A549 was chosen as a tumor cell line for initial in vitro verification because of its consistent reproducibility of the clonogenic results and a large hypoxia-induced radioresistance as has been reported in previous

publications.^{19,26,27} Another limitation of this study is that only one cell line in vitro has been used so far for the evaluation of the effect of high-LET irradiation in overcoming hypoxia-induced radioresistance. It will be important to screen in vitro several tumor types to evaluate which ones will be prime candidates for SHArc delivery and in general high-LET irradiation. Additionally, a range of oxygen levels should be investigated for a better understanding of the effect on the cell survival of high-LET_d irradiation as a function of O₂ level.

The results from the carbon LET_d-boosted IMPT plans, presented in [Supplementary Materials](#), indicate that sufficient LET_d values to overcome hypoxia-induced radioresistance can be reached with an IMPT approach at the cost of a higher beam entrance dose. Compared with classic IMPT or SHArc plans, such entrance dose, could not be suitable for OARs. From a clinical perspective, a patient representative of a glioblastoma cancer was planned with different approaches, clinical IMPT, LET_d-optimized IMPT, SHArc, and the first structure-based patient LET_d-optimized SHArc. LET-optimization strategies were performed on the GTV, where a hypoxic niche could be expected. LET_d-optimized SHArc benefits from the redistribution to the target of the high-LET_d, because of the initial energy and spot selections, as well as the novel TPS functionality to optimize LET_d, in order to reach a certain LET_d value within a selected region of interest in the target. Although the clinical IMPT plan yields superior robustness results than the other strategies, because of the potential hypoxic status of some tumor niches, it is possible that even with a reduced dose level, owing to uncertainties, the LET_d-boosted plans remain superior in terms of cell killing (and tumor control). Those results also hint that robustness optimization should be investigated further with SHArc or LET_d-optimization strategies, which are in general less robust than the non-LET optimized plans. In other words, even if the SHArc and LET_d-optimized plans seem less robust against physical uncertainties compared with clinical IMPT optimization, these plans can be more robust against biological uncertainties (eg, radioresistance, hypoxia, and RBE model differences), because of the LET redistribution toward the target.¹

These results support further research using SHArc and other LET_d-boosting strategies with carbon ions to effectively combat radioresistance factors like tumor hypoxia that could be encountered in some tumors like pancreatic adenocarcinoma and glioblastomas. Similarly, high LET_d boosting may improve the biological robustness of treatment delivery, in general, because cell response to high-LET could, in theory, become less sensitive to radioresistance factors, for example, tumor genetic background, cell-cycle phase, and tumor repair proficiency.²⁸ Nonetheless, this study focused specifically on hypoxia-related radioresistance, and future works should investigate SHArc therapy (and other LET_d-boosting strategies) in context of such endpoints.

This study involved irradiation of a central target for simplicity purposes to verify the feasibility of SHArc delivery and verify the soundness of the biological predictions. Further studies would involve target centered at off-axis points (such as P2 or P3), with or without partial arc, as well as investigation on the energy selection process to find a balance during planning between high-LET_d region size and its minimum high-LET_d value. Furthermore, SHArc delivery planning between gantry-less and heavy ion gantry systems (step-and-shoot, gantry rotation speed of ~3°/s) is envisioned to show the potential advantages and disadvantages of these 2 delivery methods.

Conclusion

The first SHArc delivery, dosimetric verification, and biological characterization were performed using carbon ion beams. Experimental evidence suggests that arc delivery with carbon ions is effective in minimizing the hypoxia-induced radioresistance in the high-LET_d tumor core for the studied cell line. Substantial high LET_d boosting in the target volume is made possible using SHArc delivery. The SHArc delivery technique with carbon ions may be an attractive approach for treating hypoxic tumor niches without increasing the dose in the surrounding normal tissues compared with other LET_d-boosting techniques but at the cost of a low-dose bath.

Disclosures

J.D. reports grants from CRI The Clinical Research Institute, grants from View Ray Incl., grants from Accuray International, grants from Accuray Incorporated, grants from RaySearch Laboratories AB, grants from Vision RT limited, grants from Merck Serono GmbH, grants from Astellas Pharma GmbH, grants from AstraZeneca GmbH, grants from Siemens Healthcare GmbH, grants from Solution Akademie GmbH, grants from Eromed PLC Surrey Research Park, grants from Quintiles GmbH, grants from Pharmaceutical Research Associates GmbH, grants from Boehringer Ingelheim Pharma GmbH Co, grants from PTW-Freiburg Dr Pyslau GmbH, and grants from Nanobiotix A.a., outside the submitted work. A.A. reports grants and other from Merck and EMD, grants and other from Fibrogen, other from BMS, other from Roche, and consulting activities for BioMedX and Bayer, outside the submitted work. L.G. is an employee of RaySearch Laboratories.

Acknowledgments

The authors express their gratitude to Dr Stephan Brons, Udo Bauer, and Nora Schumacher for their support in conducting the experiments for this study.

Statistical Analyses

Domenico Ivan Filosa, Filipa Baltazar, Andrea Mairani, and Thomas Tessonier were responsible for statistical analysis.

Supplementary materials

Supplementary material associated with this article can be found in the online version at doi:10.1016/j.adro.2024.101611.

References

1. Mein S, Tessonier T, Kopp B, et al. Spot-scanning hadron arc (SHArc) therapy: a study with light and heavy ions. *Adv Radiat Oncol.* 2021;6(3). <https://doi.org/10.1016/j.adro.2021.10066>.
2. Mein S, Kopp B, Tessonier T, et al. Spot-scanning hadron arc (SHArc) therapy: A proof of concept using single- and multi-ion strategies with helium, carbon, oxygen, and neon ions. *Med Phys.* 2022;49(9):6082-6097. <https://doi.org/10.1002/mp.15800>.
3. Mein S, Tessonier T, Kopp B, et al. Biological dose optimization for particle arc therapy using helium and carbon ions. *Int J Radiat Oncol Biol Phys.* 2022;114(2):334-348. <https://doi.org/10.1016/j.ijrobp.2022.04.025>.
4. Volz L, Sheng Y, Durante M, Graeff C. Considerations for upright particle therapy patient positioning and associated image guidance. *Front Oncol.* 2022;12: 930850.
5. Sørensen BS, Horsman MR. Tumor hypoxia: impact on radiation therapy and molecular pathways. *Front Oncol.* 2020;10:562.
6. Rockwell S, Dobrucki IT, Kim EY, Marrison ST, Vu V. Hypoxia and radiation therapy: past history, ongoing research, and future promise. *Curr Mol Med.* 2009;9:442-458.
7. Dokic I, Mairani A, Niklas M, et al. Next generation multi-scale biophysical characterization of high precision cancer particle radiotherapy using clinical proton, helium-, carbon- and oxygen ion beams. *Oncotarget.* 2016;7(35):56676-56689. <https://doi.org/10.18632/oncotarget.10996>.
8. Wenzl T, Wilkens JJ. Modelling of the oxygen enhancement ratio for ion beam radiation therapy. *Phys Med Biol.* 2011;56: 3251-3268.
9. Bassler N, Jäkel O, Søndergaard CS, Petersen JB. Dose-and LET-painting with particle therapy. *Acta Oncol.* 2010;49:1170-1176.
10. Kohno R, Koto M, Ikawa H, et al. High-linear energy transfer irradiation in clinical carbon-ion beam with the linear energy transfer painting technique for patients with head and neck. *Adv Radiat Oncol.* 2023;9: 101317.
11. Bassler N, Toftegaard J, Lühr A, et al. LET-painting increases tumour control probability in hypoxic tumours. *Acta Oncol (Madr).* 2014;53:25-32.
12. Fredriksson A, Glimelius L, Bokrantz R. The LET trilemma: conflicts between robust target coverage, uniform dose, and dose-averaged LET in carbon therapy. *Med Phys.* 2023;50:7338-7348.
13. Inaniwa T, Kanematsu N, Noda K, Kamada T. Treatment planning of intensity modulated composite particle therapy with dose and linear energy transfer optimization. *Phys Med Biol.* 2017;62: 5180-5197.
14. Inaniwa T, Kanematsu N, Shinoto M, Koto M, Yamada S. Adaptation of stochastic microdosimetric kinetic model to hypoxia for

- hypo-fractionated multi-ion therapy treatment planning. *Phys Med Biol.* 2021;66: 205007.
15. Li X, Liu G, Janssens G, et al. The first prototype of spot-scanning proton arc treatment delivery. *Radiother Oncol.* 2019;137: 130-136.
 16. Bertolet A, Carabe A. Proton monoenergetic arc therapy (PMAT) to enhance LETd within the target. *Phys Med Biol.* 2020;65: 165006.
 17. Schömers C, Brons S, Cee R, Peters A, Scheloske S, Haberer T. Beam properties beyond the therapeutic range at hit. *Published online.* 2022. <https://doi.org/10.18429/JACoW-IPAC2023-THPM064>.
 18. Mairani A, Magro G, Tessonnier T, et al. Optimizing the modified microdosimetric kinetic model input parameters for proton and 4He ion beam therapy application. *Phys Med Biol.* 2017;62(11): N244-N256. <https://doi.org/10.1088/1361-6560/aa6be9>.
 19. Mein S, Klein C, Kopp B, et al. Assessment of RBE-weighted dose models for carbon ion therapy toward modernization of clinical practice at HIT: in vitro, in vivo, and in patients. *Int J Radiat Oncol Biol Phys.* 2020;108(3):779-791. <https://doi.org/10.1016/j.ijrobp.2020.05.041>.
 20. Jäkel O, Hartmann GH, Karger CP, Heeg P, Rassow J. Quality assurance for a treatment planning system in scanned ion beam therapy. *Med Phys.* 2000;27:1588-1600.
 21. Yang M, Wohlfahrt P, Shen C, Bouchard H. Dual- and multi-energy CT for particle stopping-power estimation: current state, challenges and potential. *Phys Med Biol.* 2023;68.
 22. Inaniwa T, Kanematsu N, Inaniwa T. Adaptation of stochastic microdosimetric kinetic model for charged-particle therapy treatment planning. *Phys Med Biol.* 2018;63: 095011.
 23. Galonska M, Feldmeier E, Schömers C, Peters A, Haberer TA. Multi-energy trial operation of the hit medical synchrotron: accelerator model and data supply. *Published online.* 2017. <https://doi.org/10.18429/JACoW-IPAC2017-THPVA082>.
 24. Schömers C, Cee R, Feldmeier E, et al. Reacceleration of ion beams for particle therapy. *5th International Particle Accelerator Conference.* 2014.
 25. Iwata Y, Kadowaki T, Uchiyama H, et al. Multiple-energy operation with extended flattops at HIMAC. *Nucl Instruments Methods Phys Res Sect A Accel Spectrometers, Detect Assoc Equip.* 2010;624:33-38.
 26. Klein C, Dokic I, Mairani A, et al. Overcoming hypoxia-induced tumor radioresistance in non-small cell lung cancer by targeting DNA-dependent protein kinase in combination with carbon ion irradiation. *Radiat Oncol.* 2017;12(1). <https://doi.org/10.1186/s13014-017-0939-0>.
 27. Liew H, Klein C, Zenke FT, et al. Modeling the effect of hypoxia and DNA repair inhibition on cell survival after photon irradiation. *Int J Mol Sci Published online.* 2019. <https://doi.org/10.3390/ijms20236054>.
 28. Karger CP, Glowa C, Peschke P, Kraft-Weyrather W. The RBE in ion beam radiotherapy: in vivo studies and clinical application. *Z Med Phys.* 2021;31:105-121.